ISA Transactions 137 (2023) 111–121

Contents lists available at ScienceDirect

ISA Transactions

journal homepage: www.elsevier.com/locate/isatrans

Research article

Event-based formation control for multiple unmanned aerial vehicles under directed topology☆

Tingting Yin, Zhou Gu *, Shen Yan

College of Mechanical & Electronic Engineering, Nanjing Forestry University, Nanjing 210037, PR China

ARTICLE INFO

Article history:
Received 9 June 2022
Received in revised form 2 January 2023
Accepted 14 January 2023
Available online 20 January 2023

Keywords:
Formation control
Unmanned aerial vehicles
Event-triggered scheme
Cyber attacks

ABSTRACT

This paper focuses on the problem of formation control for multiple unmanned aerial vehicles (UAV) subject to cyber attacks by a novel event-triggered communication scheme. An average method is introduced to design the triggering condition of this communication scheme, by which the amount of wrong triggering events caused by the sudden change of system states is greatly decreased, thereby saving a great deal of network bandwidth and reducing network congestion. Considering cyber attacks, a new event-based formation control strategy is developed for multi-UAV systems under directed topology by utilizing a control compensation approach. Sufficient conditions for the multi-UAV system to achieve the desired formation are acquired. Finally, a simulation example is undertaken to demonstrate the effectiveness of the theoretical results.

1. Introduction

The research on multiple unmanned aerial vehicles (UAV) have received great attention due to its widespread applications, such as information collection and offensive maneuvers in restricted environments, and moving targets tracking in military operations [1–5]. A critical issue of multiple unmanned aerial vehicles is the formation problem, which is to develop an appropriate control strategy via interactions between the neighboring UAVs to achieve the desired formation. In the past years, the formation problem of multiple UAVs has become a hot topic and received considerable attention, see [6–8] and the references therein. For example, the authors in [7] investigate the formation circumnavigation for UAVs using an adaptive backstepping method. A relative localization algorithm is proposed for multi-UAV formation control in [8]. The authors focus on the formation control for event-triggered multi-UAV systems in [9]. However, the above results involve time-invariant formations, which usually cannot meet the actual requirements under various circumstances, such as the changing environment, obstacle avoidance, and other complicated missions. Accordingly, it motivates numerous researches on time-varying formation control. The time-varying formation tracking control for multi-UAV systems is investigated in [10], where the communication topography graph among UAVs is undirected. The problem of time-varying formation tracking for leader-following multi-UAV systems is addressed in [11] by using a sliding mode control method. In [12], the issue of feedback formation tracking is studied for multi-UAV systems with multiple leaders. It can be concluded from the above achievements that UAVs discussed in the existing literature are divided into leader-following and leaderless ones based on whether or not to contain leaders. Notice that the control strategies in [10,13] depend on the symmetric Laplacian matrix related to the undirected communication graph, which cannot be extended to handle the situation with directed graphs. Consequently, it is meaningful and challenging work to investigate the problem of formation tracking control for multi-UAV systems under directed topology. This is our main motivation to promote this research.

To achieve the desired formation, all UAVs in a multi-UAV system realize information interaction over a shared network. As is known to all, the communication resource of the network is limited [14–16]. Therefore, designing an effective data transmission mechanism is crucial to save bandwidth and improve resource utilization while maintaining satisfactory system performance [17–19]. For such a reason, significant efforts have been devoted to analyzing the networked multi-UAV systems [20–24]. Time-triggered scheme is usually adopted in networked systems, which is characterized by working at predetermined points in time. Under this scheme, the desired performance of multi-UAV system can be kept even if the system suffers from external disturbances. However, if the system reaches asymptotic stability,

☆ This work was supported by the National Natural Science Foundation of China under Grant 62273183, 62103193 and 62022044, and in part by the Natural Science Foundation of Jiangsu Province of China under Grant BK20200769.

* Corresponding author.
E-mail addresses: yintingting@njfu.edu.cn (T. Yin), guzhou@njfu.edu.cn (Z. Gu), yanshen@njfu.edu.cn (S. Yan).

https://doi.org/10.1016/j.isatra.2023.01.018
0019-0578/

it may produce numerous redundant data, which increases the network bandwidth load. To deal with this problem, a discrete event-triggered scheme (ETS) is developed in [25] for the first time and is widely available in the published achievements. This scheme impels the sampled measurements to be transmitted over the network only when the predetermined triggering condition is sustained. As a result, the use of ETS results in improving the utilization of network bandwidth and lessening the waste of computation and communication resources. Inspired by such an ETS, some improved communication schemes have been developed over the past decades, including dynamic ETS [21], hybrid triggered scheme [24], memory-based ETS [26,27]. Large quantities of outcomes have been achieved in the last years, including state estimation [28], filters [29,30] and controller design [21,31]. For example, the authors in [21] propose one kind of asynchronous controller for multiagent systems by implementing the dynamic ETS. Using the memory-based ETS, the secure control problem is addressed for active suspension systems under deception attacks in [31]. The application of event-triggered communication scheme brings a lower data release rate and less energy consumption without the degradation of system performance. Given this, it is of theoretical and practical significance to develop an appropriate data communication mechanism for the multi-UAV system, which motivates the current work.

In the study of multi-UAV systems, many efforts have been made to handle the network security issue of the networked multi-UAV systems owing to the reliability requirements for data transmission during the past decades [32–35]. So far, there has been quite a few results on cyber attacks because cyber-attacks are the most formidable barrier to smooth data communication of each UAV in a multi-UAV system, see [36–39] for replay attacks, [40–44] for denial-of-service (DoS) attacks, and [45–49] for deception attacks. For example, the fusion estimation issue is discussed for cyber–physical systems in the presence of replay attacks in [38]. The problem of the input-based event-triggering consensus of multiagent systems under DoS attacks is investigated in [41]. In [47], the authors focus on fault-tolerant consensus tracking for multiagent systems by taking deception attacks into account. Considering such a type of cyber-attack, the secure impulsive synchronization control is addressed for multiagent systems in [48]. The related work is still an ongoing research topic, particularly for multi-UAV systems with cyber-attacks; for example, it is a promising work to develop the formation control strategies in the presence of deception attacks, which impels this study to a considerable extent.

Based on the above analysis, this paper studies the formation control for multi-UAV systems subject to cyber attacks. The contributions of this research can be unfolded in the following aspects:

(I) A new event-triggered scheme is designed for multi-UAV systems, under which an average of the current input signal and the latest triggering signal is introduced to develop its triggering condition. Compared with the existing communication mechanisms [19,25], the proposed ETS can further reduce the number of wrong triggering events aroused by the accidentally sudden state variation;

(II) A novel event-based formation control strategy is developed for multi-UAV systems under cyber attacks by using a control compensation method. Compared with the existing study on multi-UAV systems without cyber-attacks [9,10], the influence of cyber-attacks is taken into account in this study, which is closer to the actual situation. Besides, the use of our proposed control strategy with a compensation term contributes to better accuracy and shorter time of the multi-UAV system to realize the desired formation than the formation control method in [35].

The rest of this paper is organized as follows. Section 2 gives the preliminaries and problem formulation for the studied multi-UAV system. The main results of the formation control for multi-UAV systems are exhibited in Section 3. Section 4 provides a simulation example for testifying the feasibility of the obtained results. Finally, the research is concluded in Section 5.

Notation: The set of m_1-dimensional Euclidean space is denoted as R^{m_1}; the identity matrix and the zero matrix are denoted as I and 0, respectively. $I_{n_1\times n_2}$ ($0_{n_1\times n_2}$) denotes the $n_1 \times n_2$-dimensional identity (zero) matrix; if $n_1 = n_2$, it is abbreviated as I_{n_1} (0_{n_1}). Symbol $*$ of a symmetric matrix is the term indicated by symmetry. Matrix $\mathcal{X} > 0$ denotes that $\mathcal{X}$ is real symmetric positive definite. $\mathrm{sym}\{\mathcal{X}\}$ stands for $\mathcal{X} + \mathcal{X}^T$. $\mathcal{E}(\cdot)$ denotes the mathematical expectation.

2. Preliminaries and problem formulation

2.1. Preliminaries

A directed graph $\mathbb{F} = (\mathbb{W}, \mathbb{E}, \mathbb{B})$ describes the communication topology among N UAVs, in which $\mathbb{W} = \{1, 2, \ldots, N\}$ and $\mathbb{E} \subseteq \{(i, j), i, j \in \mathbb{W}\}$ indicate the set of nodes and edges, respectively. $\mathbb{B} = [b_{ij}]$ is the weighted adjacency of $\mathbb{F}$, where $b_{ii} = 0$, $b_{ij} = 1$ $\Leftrightarrow$ edge $(j, i) \in \mathbb{E}$; otherwise, $b_{ij} = 0$. If the ith UAV can acquire the jth UAV's information, $(j, i) \in \mathbb{E}$. Denote the Laplacian matrix as $\mathfrak{L} = \mathbb{D} - \mathbb{B}$, where the in-degree matrix is represented as $\mathbb{D} = \mathrm{diag}\{\mathbf{d}_1, \mathbf{d}_2, \ldots, \mathbf{d}_N\}$, wherein $\mathbf{d}_i = \Sigma_{j\in\mathcal{B}_i} b_{ij}$ for the ith UAV. The set $\mathcal{B}_i = \{j|(i, j) \in \mathbb{E}\}$ consists of all neighbors for the ith UAV.

2.2. Problem description

The configuration of a quadrotor UAV consists of four rotors and a rigid cross frame. The quadrotor UAV's motion (including position motion in x, y and z directions, and attitude motion in pitch, roll and yaw) can be realized via the appropriate combination of these four rotors [11]. Only the trajectory-loop of the UAV are taken into consideration in this research. The attitude tracking can be achieved through autopilot. The 3-DOF rotational motions of the UAV can be described as [5]:

$$\begin{cases} \dot{x}_{i\vartheta}(t) = x_{iv}(t), \\ \dot{x}_{iv}(t) = -g e_{\mathrm{x}} + \frac{h_i}{m_i}\mathcal{M} e_{\mathrm{x}}, \end{cases} \tag{1}$$

where $x_{i\vartheta}(t) = [x_{i\vartheta X}(t), x_{i\vartheta Y}(t), x_{i\vartheta Z}(t)]^T \in \mathrm{R}^3$ and $x_{iv}(t) = [x_{ivX}(t), x_{ivY}(t), x_{ivZ}(t)]^T \in \mathrm{R}^3$ denotes the position and the velocity of the UAV in world frame, namely North East Down coordinate frame; $e_{\mathrm{x}} = [0 \;\; 0 \;\; 1]^T$; g denotes the gravitational acceleration; m_i represents the UAV's mass; $\mathcal{M}$ stands for the coordinate transition matrix from the body frame to the world frame for the UAV, which is expressed as

$$\mathcal{M} = \begin{bmatrix} \mathbf{c}_\theta \mathbf{c}_\psi & \mathbf{s}_\theta \mathbf{c}_\psi \mathbf{s}_\phi - \mathbf{c}_\phi \mathbf{s}_\psi & \mathbf{s}_\theta \mathbf{c}_\phi \mathbf{c}_\psi + \mathbf{s}_\phi \mathbf{s}_\psi \\ \mathbf{c}_\theta \mathbf{s}_\psi & \mathbf{s}_\theta \mathbf{s}_\phi \mathbf{s}_\psi + \mathbf{c}_\phi \mathbf{c}_\psi & \mathbf{s}_\theta \mathbf{c}_\phi \mathbf{s}_\psi - \mathbf{c}_\psi \mathbf{s}_\theta \\ -\mathbf{s}_\phi & \mathbf{c}_\theta \mathbf{s}_\phi & \mathbf{c}_\theta \mathbf{c}_\phi \end{bmatrix},$$

where $\mathbf{s}_{(\cdot)}$ and $\mathbf{c}_{(\cdot)}$ denote $\sin(\cdot)$ and $\cos(\cdot)$ respectively; the Euler angles in the world frame are represented as ϕ, θ, ψ; h_i is the elevating force in the UAV's body frame. Denote $u_i(t) = -g e_{\mathrm{x}} + \frac{h_i}{m_i}\mathcal{M} e_{\mathrm{x}}$, $x_i(t) = [x_{i\vartheta}^T(t), x_{iv}^T(t)]^T$, then, motivated by [10], the translational equation of the UAV could be converted into the following dynamic equation:

$$\dot{x}_i(t) = A x_i(t) + B u_i(t), \tag{2}$$

where $A = \begin{bmatrix} 0 & I_3 \\ 0 & 0 \end{bmatrix}$, $B = \begin{bmatrix} 0 \\ I_3 \end{bmatrix}$. In the multi-UAV system, the 0th UAV is set as leader UAV, who generates the reference trajectory, and UAVs $1, 2, 3, \ldots, N$ are denoted as follower UAVs to track the reference trajectory.

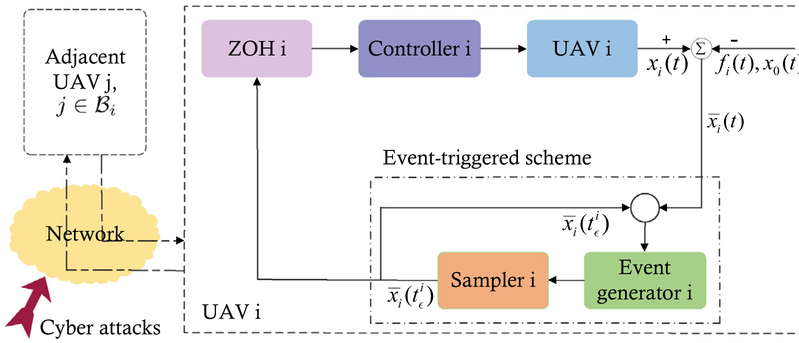

Fig. 1. Framework of event-based control for the ith UAV.

Assumption 1. There has been a directed spanning tree in the graph $\mathbb{F}$ of multi-UAV systems, in which the root node is the 0th UAV.

Consider a time-varying formation of followers described by $f(t) = [f_1^T(t), f_2^T(t), \ldots, f_N^T(t)]^T$ with $f_i(t) = [f_{i\vartheta}(t), f_{iv}(t)]^T$ and $f_{iv}(t) = \dot{f}_{i\vartheta}(t)$. $f_{i\vartheta}(t)$ ($f_{iv}(t)$) is the relative position (velocity) variable for the ith UAV, $i \in \{1, 2, \ldots, N\} \triangleq \mathrm{G}$. Then, the desired state of the ith UAV can be expressed as $\Upsilon_i(t) = f_i(t) + x_0(t)$, where $\Upsilon_i(t) = [\Upsilon_{i\vartheta}^T(t), \Upsilon_{iv}^T(t)]^T$, $\Upsilon_{iv}(t) = \dot{\Upsilon}_{i\vartheta}(t)$. Moreover, the formation error of the ith UAV is denoted as $\bar{x}_i(t) = x_i(t) - \Upsilon_i(t)$.

This study aims at proposing a control strategy for system (2) to realize the formation control. In the absence of cyber-attacks, the following control strategy is developed for the ith UAV without event-triggered scheme:

$$u_i(t) = -K_1 c_i \bar{x}_i(t) + u_{ik}(t) + \dot{\Upsilon}_{iv}(t) - B^+ A \Upsilon_i(t), \tag{3}$$

wherein

$$u_{ik}(t) = -K_2 \sum_{j \in \mathcal{B}_i} b_{ij} \left[x_i(t) - f_i(t) - (x_j(t) - f_j(t)) \right],$$

where c_i describes whether or not to has a communication link between the ith UAV and the 0th UAV. $c_i = 1$ denotes that the ith UAV can receive the information of the 0th UAV; otherwise, $c_i = 0$. $\dot{\Upsilon}_{iv}(t)$ is the desired acceleration, which can be acquired in advance. $B^+ = (B^T B)^{-1} B^T$. K_1, K_2 are controller gains. $\mathcal{B}_i$ and b_{ij} are given in Section 2.1.

Remark 1. In (3), a compensation term $B^+ A \Upsilon_i(t)$ is utilized, which is determined by the desired state of the ith UAV. The usage of the effective compensation term can bring better accuracy and shorter time of the multi-UAV system to realize the formation than the conventional control approach [35] without using the compensation term.

Fig. 1 exhibits the framework of event-triggered control for the ith UAV under cyber attacks. In this framework, an ETS is introduced to ease the bandwidth load of the network. Under this scheme, an average method is adopted to cut down wrong triggering events caused by the sudden change of system states. Now the triggering condition of the designed ETS is given as follows: For $t \in [t^i_\epsilon, t^i_{\epsilon+1})$,

$$\phi_i \zeta_i^T(t) \Omega_i \zeta_i(t) < \eta_i^T(t) \Omega_i \eta_i(t), \tag{4}$$

where $\zeta_i(t) = \frac{1}{2}\left[\bar{x}_i(t^i_\epsilon) + \bar{x}_i(t)\right]$, $\eta_i(t) = \zeta_i(t^i_\epsilon) - \bar{x}_i(t) = \frac{1}{2}\left[\bar{x}_i(t^i_\epsilon) - \bar{x}_i(t)\right]$; $\phi_i \in [0, 1)$, $\Omega_i > 0$ is the weight matrix to be designed; and $\bar{x}_i(t^i_\epsilon)$ is the latest transmitted signal; the current input signal $\bar{x}_i(t)$ can be transmitted over the network only when the triggering condition (4) is satisfied. Denote the set of triggering instants for the ith UAV as $\{t^i_0, t^i_1, \ldots, t^i_\epsilon, t^i_{\epsilon+1}, \ldots\}$, wherein $t^i_0 < t^i_1 < \cdots < t^i_\epsilon < t^i_{\epsilon+1} < \cdots$, $t^i_0 = 0$, $i \in \mathrm{G}$, $\epsilon \in \{0, 1, 2, \ldots\}$. It is worth noticing that the 0th UAV is not triggered in this study.

Furthermore, the event-triggered signal is expressed as

$$\bar{x}_i(t^i_\epsilon) = \bar{x}_i(t) + 2\eta_i(t). \tag{5}$$

Remark 2. Notice that an average $\zeta_i(t)$ of the current input signal $\bar{x}_i(t)$ and the latest triggering signal $\bar{x}_i(t^i_\epsilon)$ is considered when we design the triggering condition of ETS (4). Compared to the existing event-triggered schemes without adopting the average method, our proposed ETS can generate fewer wrong triggering events, and smooth the releasing period, especially in the case of sudden state variation. At the same time, the performance of multi-UAV systems can be guaranteed.

Notice that the performance of multi-UAV systems relies on whether each UAV realizes reliable information interaction via network or not to a great extent. In view of this, cyber attacks, as one of the biggest threats to network security, should be considered, shown in Fig. 1. In this study, we consider deception attacks. When the deception attack takes place, attack signal $\varepsilon_j(t)$ will replace the normal transmitted signal. For the purpose of describing such a cyber-attack, a Bernoulli random variable $\delta_j(t) \in \{0, 1\}$ with its expectation $\bar{\delta}_j$ and mathematical variance ρ_j^2 is applied in this study. Then, the real control input of the ith UAV, which results from the jth UAV via the network with cyber-attacks, can be expressed as

$$\hat{\bar{x}}_j(t) = \delta_j(t)\varepsilon_j(t) + (1 - \delta_j(t))\bar{x}_j(t^j_{\epsilon'}), \tag{6}$$

where $\bar{x}_j(t^j_{\epsilon'})$ is given in (5) and $\varepsilon_j(t)$ is given in (7); $\bar{x}_j(t^j_{\epsilon'})$ denotes the latest transmitted signal from the jth UAV, and $\epsilon' \triangleq \mathrm{argmin}_{\epsilon'}\{t - t^j_{\epsilon'} | t > t^j_{\epsilon'}, \epsilon' = 0, 1, 2, 3, \ldots\}$. The independent variable $\delta_j(t)$ satisfies $\delta_j(t) \neq \delta_i(t)$ for $j \neq i$, $i, j \in \mathrm{G}$.

In this study, the attack signal $\varepsilon_j(t)$ is considered in the form as follows:

$$\varepsilon_j(t) = \xi_j(t) - \bar{x}_j(t), \tag{7}$$

where $\xi_j(t)$ is selected so as to satisfy the following condition: given a real matrix M_j and a real constant $\theta \geq 0$, inequality (8) holds.

$$(\xi_j(t) - M_j \bar{x}_j(t))^T (\xi_j(t) - M_j \bar{x}_j(t)) \leq \theta^2 \bar{x}_j^T(t) \bar{x}_j(t). \tag{8}$$

Remark 3. From (6), it can be observed that when $\delta_j(t) = 1$, $\hat{\bar{x}}_j(t) = \varepsilon_j(t)$, which implies that the transmitted signal $\bar{x}_j(t^j_{\epsilon'})$ is replaced by the attack signal $\varepsilon_j(t)$; when $\delta_j(t) = 0$, $\hat{\bar{x}}_j(t) = \bar{x}_j(t^j_{\epsilon'})$, which indicates that cyber-attacks do not occur and the transmitted signal $\bar{x}_j(t^j_{\epsilon'})$ can reach the controller side.

Remark 4. Cyber attacks may be more complex and diverse in an actual environment. However, this study focuses on the problem of event-based formation control for multi-UAV systems. More accurate modeling of attacks will be explored in future research.

Based on the ETS in (4) and the cyber-attack in (6), the controller (3) of the ith UAV is actually piecewise, that is, $u_i(t) = u_i(t_\epsilon^i)$ for $t \in [t_\epsilon^i, t_{\epsilon+1}^i)$. Then, the controller (3) for the ith UAV subject to cyber-attacks can be expressed as follows:

$$u_i(t) = -K_1 c_i \bar{x}_i(t_\epsilon^i) + u_{ik}(t) + \dot{\Upsilon}_{iv}(t) - B^+ A \Upsilon_i(t), \tag{9}$$

where $u_{ik}(t) = -K_2 \sum_{j\in\mathcal{B}_i} b_{ij}\left[\bar{x}_i(t_\epsilon^i) - \hat{\bar{x}}_j(t)\right]$.

Notice that $\bar{x}_i(t) = x_i(t) - f_i(t) - x_0(t)$, taking its derivation and combining (2), (5)–(7), (9), then, the following tracking error system can be obtained by using Kronecker product:

$$\begin{aligned}\dot{\bar{x}}(t) =&(\tilde{A} - \tilde{C}\tilde{K}_1 - \tilde{L}\tilde{K}_2)\bar{x}(t) - 2(\tilde{C}\tilde{K}_1 + \tilde{L}\tilde{K}_2)\eta(t)\\ &- \delta(t)\tilde{W}\tilde{K}_2[\xi(t) - 2\bar{x}(t) - 2\eta(t)],\end{aligned} \tag{10}$$

where $\tilde{A} = I_N \otimes A$, $\tilde{K}_1 = I_N \otimes K_1$, $\tilde{K}_2 = I_N \otimes K_2$, $\tilde{C} = \mathbb{C} \otimes B$, $\tilde{L} = \mathfrak{L} \otimes B$, $\tilde{W} = \mathbb{W} \otimes B$, $\delta(t) = \mathrm{diag}\{\delta_1(t), \delta_2(t), \ldots, \delta_N(t)\}$, and $\bar{x}^T(t) = [\bar{x}_1^T(t), \bar{x}_2^T(t), \ldots, \bar{x}_N^T(t)]$, $\eta^T(t) = [\eta_1^T(t), \eta_2^T(t), \ldots, \eta_N^T(t)]$, $\xi^T(t) = [\xi_1^T(t), \xi_2^T(t), \ldots, \xi_N^T(t)]$.

3. Main results

The stability analysis for the formation control of multi-UAV systems under cyber-attacks will be given in this section.

Theorem 1. *Given scalars $\phi_i \in (0, 1)$, $\bar{\delta}_i \in (0, 1)$, $\theta \geq 0$, K_1 and K_2, system (2) with the ETS (4) and the controller (9) is asymptotically stable if there are matrices $P > 0$, $\Omega_i > 0$, and M_i $(i \in \mathrm{G})$ such that the following inequality holds:*

$$\Psi = \begin{bmatrix} \Pi_{11} & * & * \\ \Pi_{21} & \Pi_{22} & * \\ \Pi_{31} & 0 & \Pi_{33} \end{bmatrix} < 0, \tag{11}$$

where

$$\begin{aligned}\Pi_{11} =&sym\{\bar{P}\tilde{A} - \bar{P}\tilde{C}\tilde{K}_1 - \bar{P}\tilde{L}\tilde{K}_2 + 2\bar{P}\bar{\delta}\tilde{W}\tilde{K}_2\}\\ &- \bar{\delta}\bar{M}^T\bar{P}\bar{M} + \bar{\delta}\theta^2\bar{P} + \phi\Omega,\\ \Pi_{21} =& -2\tilde{K}_1^T\tilde{C}^T\bar{P} - 2\tilde{K}_2^T\tilde{L}^T\bar{P} + 2\tilde{K}_2^T\tilde{W}^T\bar{\delta}\bar{P} + \phi\Omega,\\ \Pi_{22} =& -\Omega + \phi\Omega, \Pi_{31} = -\tilde{K}_2^T\tilde{W}^T\bar{\delta}\bar{P} + \bar{\delta}\bar{P}\bar{M},\\ \Pi_{33} =& -\bar{\delta}\bar{P}, \tilde{K}_1 = I_N \otimes K_1, \tilde{K}_2 = I_N \otimes K_2,\\ \phi =&\phi_f \otimes I_{2n}, \phi_f = diag\{\phi_1, \phi_2, \ldots, \phi_N\},\\ \bar{\delta} =&\bar{\delta}_f \otimes I_{2n}, \bar{\delta}_f = diag\{\bar{\delta}_1, \bar{\delta}_2, \ldots, \bar{\delta}_N\},\\ \Omega =&diag\{\Omega_1, \Omega_2, \ldots, \Omega_N\},\\ \bar{M} =&diag\{M_1, M_2, \ldots, M_N\}.\end{aligned}$$

Proof. The proof can be compartmentalized into two steps as follows: Step I gives the stability analysis of system (10), and Step II presents the avoidance of the Zeno behavior in the proposed ETS.

Step I: Choose the following Lyapunov function for system (10):

$$V(\bar{x}(t)) = \bar{x}^T(t)\bar{P}\bar{x}(t), \tag{12}$$

where $\bar{P} = I_N \otimes P$.

Calculating the derivation and the mathematical expectation of (12) yields that

$$\begin{aligned}\mathcal{E}\left\{\dot{V}(\bar{x}(t))\right\} =&2\bar{x}^T(t)\bar{P}\left\{(\tilde{A} - \tilde{C}\tilde{K}_1 - \tilde{L}\tilde{K}_2)\bar{x}(t)\right.\\ &-\bar{\delta}\tilde{W}\tilde{K}_2[\xi(t) - 2\bar{x}(t) - 2\eta(t)]\\ &\left.-2(\tilde{C}\tilde{K}_1 + \tilde{L}\tilde{K}_2)\eta(t)\right\}.\end{aligned} \tag{13}$$

According to inequality (4), one can easily obtain that

$$\Xi_1(t) - \eta^T(t)\Omega\eta(t) < 0, \tag{14}$$

where $\Xi_1(t) = [\bar{x}(t) + \eta(t)]^T\phi\Omega[\bar{x}(t) + \eta(t)]$.

It follows from inequality (8) that there exists a symmetric matrix $\bar{P}$ so as to satisfy the condition as follows:

$$\theta^2\bar{x}^T(t)\bar{P}\bar{x}(t) - \Xi_2(t) \leq 0, \tag{15}$$

where $\Xi_2(t) = [\xi(t) - \bar{M}\bar{x}(t)]^T\bar{P}[\xi(t) - \bar{M}\bar{x}(t)]$.

Combining inequalities (13)–(15) and utilizing Schur complement yield that

$$\mathcal{E}\left\{\dot{V}(\bar{x}(t))\right\} \leq \chi^T(t)\Psi\chi(t), \tag{16}$$

where $\chi(t) = [\bar{x}^T(t)\ \ \eta^T(t)\ \ \xi^T(t)]^T$. It follows from $\Psi < 0$ that $\mathcal{E}\left\{\dot{V}(\bar{x}(t))\right\} < 0$. As a result, the conclusion can be drawn that system (10) is asymptotically stable if inequality (11) holds.

Step II: The discussion on the exclusion of Zeno behavior in the ETS will be presented in the form of two cases.

Case i: When system (10) approaches stable, $\bar{x}_i(t) = 0$. Under this circumstance, (4) is satisfied and $\bar{x}_i(t)$ will be transmitted via the network. Evidently, it is the last triggering behavior because both sides of inequality (4) equals to zero. Since the ETS does not work anymore when the system is stable, the Zeno behavior is avoided naturally.

Case ii: Consider the situation that $\bar{x}_i(t) \neq 0$. Due to inequality (4), we have $\lambda_{\max}(\Omega_i)\phi_i \parallel \zeta_i(t) \parallel^2 < \lambda_{\max}(\Omega_i) \parallel \eta_i(t) \parallel^2$, $\zeta_i(t) = \frac{1}{2}\left[\bar{x}_i(t_\epsilon^i) + \bar{x}_i(t)\right]$. Denoting $\kappa = \arg\max_i \parallel \eta_i(t) \parallel (i \in \mathrm{G})$ yields that $\parallel \eta_i(t) \parallel \leq \parallel \eta(t) \parallel$, then, one has $\frac{\|\eta_\kappa(t)\|}{\|\bar{x}_\kappa(t)\|} \leq \frac{\sqrt{N}\|\eta(t)\|}{\|\bar{x}(t)\|}$. Once the ETS works, one can get $\eta_i(t) = 0$. Consequently, denote ε_κ as the time interval for $\parallel \eta_\kappa(t) \parallel / \parallel \bar{x}_\kappa(t) \parallel$ growing from 0 to ϕ_i, and ε^* as the time interval from 0 to $\sqrt{N} \parallel \eta(t) \parallel / \parallel \bar{x}(t) \parallel$.

Due to $\eta_i(t) = \frac{1}{2}[\bar{x}_i(t_\epsilon^i) - \bar{x}_i(t)]$, for any certain instant t_ϵ^i, $\dot{\bar{x}}_i(t_\epsilon^i) = 0$, $\dot{\eta}_i(t) = -\frac{1}{2}\dot{\bar{x}}_i(t)$. Then, one has

$$\begin{aligned}\frac{\mathrm{d}}{\mathrm{d}t}\frac{\parallel \eta(t) \parallel}{\parallel \bar{x}(t) \parallel} =& -\frac{\eta^T(t)\dot{\bar{x}}(t)}{2 \parallel \eta(t) \parallel\parallel \bar{x}(t) \parallel} - \frac{\eta(t)\bar{x}^T(t)\dot{\bar{x}}(t)}{2 \parallel \bar{x}(t) \parallel^2\parallel \bar{x}(t) \parallel}\\ \leq& \left(1 + \frac{\parallel \eta(t) \parallel}{\parallel \bar{x}(t) \parallel}\right)\\ &\left(\parallel \Lambda_1 \parallel + \parallel \Lambda_2 \parallel \frac{\parallel \eta(t) \parallel}{\parallel \bar{x}(t) \parallel} + \varphi_{\sup}\right),\end{aligned} \tag{17}$$

where $\Lambda_1 = \tilde{A} - \tilde{C}\tilde{K}_1 - \tilde{L}\tilde{K}_2 + 2\bar{\delta}\tilde{W}\tilde{K}_2$, $\Lambda_2 = -2(\tilde{C}\tilde{K}_1 + \tilde{L}\tilde{K}_2 - \bar{\delta}\tilde{W}\tilde{K}_2)$; and $\varphi_{\sup} = \sup\left\{\frac{\|-\bar{\delta}\tilde{W}\tilde{K}_2\xi(t)\|}{\|\bar{x}(t)\|}\right\}$ $(\parallel \bar{x}(t) \parallel \neq 0)$.

Defining $\nu = \parallel \eta(t) \parallel / \parallel \bar{x}(t) \parallel$, (17) can be expressed as $\dot{\nu} \leq (1 + \nu)\left(\parallel \Lambda_1 \parallel + \parallel \Lambda_2 \parallel \nu + \varphi_{\sup}\right)$. Assume that $\varpi(t, \varpi_0)$ is the solution of $\dot{\varpi} = (1 + \varpi)\left(\parallel \Lambda_1 \parallel + \parallel \Lambda_2 \parallel \varpi + \varphi_{\sup}\right)$ and $\varpi(0, \varpi_0) = \varpi_0$. According to the aforementioned analysis, one can conclude that $\nu \leq \varpi(t, \varpi_0)$. It is supposed that $\eta(t)$ and ϖ_0 are equal to 0 at the initial time. In that way, the smallest time interval can be acquired by integrating the both sides of the following equality: $\mathrm{d}t = \frac{\mathrm{d}\varpi}{(1+\varpi)\left(\|\Lambda_1\|+\|\Lambda_2\|\varpi+\varphi_{\sup}\right)}$. Then, we can obtain

$$\begin{aligned}\varepsilon =&\frac{1}{\parallel \Lambda_1 \parallel + \parallel \Lambda_2 \parallel \varpi + \varphi_{\sup}}\\ &\times \ln\left[\frac{(\parallel \Lambda_1 \parallel + \varphi_{\sup})\varpi(t, 0) + \parallel \Lambda_1 \parallel + \varphi_{\sup}}{\parallel \Lambda_2 \parallel \varpi(t, 0) + \parallel \Lambda_1 \parallel + \varphi_{\sup}}\right].\end{aligned} \tag{18}$$

Setting $\varpi(t^*, 0) = \sqrt{\sum_{i=1}^N \phi_i / N}$ yields the smallest time interval

$$\begin{aligned}\varepsilon^* =&\frac{1}{\parallel \Lambda_1 \parallel + \parallel \Lambda_2 \parallel \varpi + \varphi_{\sup}}\\ &\times \ln\left[\frac{(\parallel \Lambda_1 \parallel + \varphi_{\sup})\varpi(t^*, 0) + \parallel \Lambda_1 \parallel + \varphi_{\sup}}{\parallel \Lambda_2 \parallel \varpi(t^*, 0) + \parallel \Lambda_1 \parallel + \varphi_{\sup}}\right].\end{aligned} \tag{19}$$

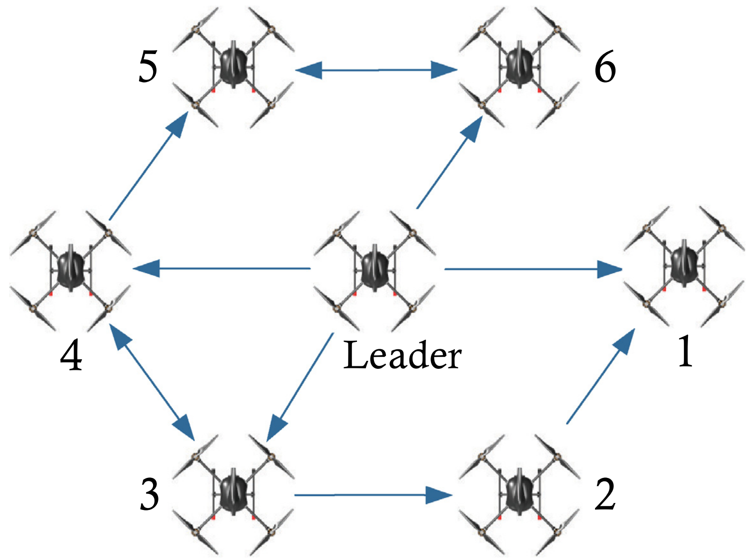

Fig. 2. Communication topology of the multi-UAV system.

Based on the above analysis and discussion, it is easy to obtain that $0 < \varepsilon^* \leq \varepsilon_\kappa$, which indicates the Zeno behavior in the proposed ETS can be excluded. That ends the proof. ■

Sufficient conditions are obtained in Theorem 1 when the asymptotical stability of the overall system (10) is ensured. Based on this, the controller gains and the weight matrices of the proposed ETS are obtained in what follows.

Theorem 2. *Given scalars $\phi_i \in (0,1)$, $\bar{\delta}_i \in (0,1)$, $\theta \geq 0$, system (2) with the ETS (4) and the controller (9) is asymptotically stable if there are matrices $\tilde{\Omega}_i > 0$, Y, $\bar{X}$, and M_i ($i \in$ G) such that the following linear matrix inequality holds:*

$$\tilde{\Psi} = \begin{bmatrix} \tilde{\Pi}_{11} & * & * \\ \tilde{\Pi}_{21} & \tilde{\Pi}_{22} & * \\ \tilde{\Pi}_{31} & 0 & \tilde{\Pi}_{33} \end{bmatrix} < 0, \tag{20}$$

where

$$\begin{aligned} \tilde{\Pi}_{11} =& sym\{\bar{A}\tilde{X} - \tilde{C}\tilde{Y}_1 - \tilde{L}\tilde{Y}_2 + 2\bar{\delta}\tilde{W}\tilde{Y}_2\} \\ & - \bar{M}^T\bar{\delta}_1\tilde{X}\bar{M} + \bar{\delta}\theta^2\tilde{X} + \phi\tilde{\Omega}, \\ \tilde{\Pi}_{21} =& -2\tilde{Y}_1^T\tilde{C}^T - 2\tilde{Y}_2^T\tilde{L}^T + 2\tilde{Y}_2^T\tilde{W}^T\bar{\delta} + \phi\tilde{\Omega}, \\ \tilde{\Pi}_{22} =& -\tilde{\Omega} + \phi\tilde{\Omega}, \tilde{\Pi}_{31} = -\tilde{Y}_2^T\tilde{W}^T\bar{\delta} + \bar{\delta}\bar{M}\tilde{X}, \\ \tilde{\Pi}_{33} =& -\bar{\delta}\tilde{X}, \tilde{\Omega} = diag\{\tilde{\Omega}_1, \tilde{\Omega}_2, \ldots, \tilde{\Omega}_N\}. \end{aligned}$$

Furthermore, the parameters of the controller and the ETS are designed as

$$K_1 = \mathrm{Y}_1\bar{X}^{-1}, K_2 = \mathrm{Y}_2\bar{X}^{-1}, \Omega_i = \bar{X}^{-1}\tilde{\Omega}_i\bar{X}^{-1}, i \in \mathrm{G}. \tag{21}$$

Proof. Define $\bar{X} = P^{-1}$, $\mathrm{Y}_1 = K_1\bar{X}$, $\mathrm{Y}_2 = K_2\bar{X}$, $\tilde{X} = I_N \otimes \bar{X}$, $\tilde{Y}_1 = I_N \otimes \mathrm{Y}_1$, $\tilde{Y}_2 = I_N \otimes \mathrm{Y}_2$. Denote $\Gamma_a = \mathrm{diag}\{\tilde{X}, \tilde{X}, \tilde{X}\}$ and $\tilde{\Omega}_i = \bar{X}\Omega_i\bar{X}$, then, multiplying two sides of Ψ with Γ_a and Γ_a^T yields that $\tilde{\Psi} < 0$. According to the analysis of Theorem 1, system (10) is asymptotically stable. Consequently, the parameters of the controller and the ETS can be gained by solving linear matrix inequality (20) and using the equalities in (21). That ends the proof. ■

4. Simulation example

The effectiveness of the proposed method will be testified in this section. Assume that there are six follower UAVs and one leader in a multi-UAV system whose communication topology is presented in Fig. 2. From this topology graph, it can be obtained that $\mathbb{C} = \mathrm{diag}\{1, 0, 1, 1, 0, 1\}$ and Laplacian matrix:

$$\mathfrak{L} = \begin{bmatrix} 1 & -1 & 0 & 0 & 0 & 0 \\ 0 & 1 & -1 & 0 & 0 & 0 \\ 0 & 0 & 1 & -1 & 0 & 0 \\ 0 & 0 & -1 & 1 & 0 & 0 \\ 0 & 0 & -1 & 0 & 2 & -1 \\ 0 & 0 & 0 & 0 & -1 & 1 \end{bmatrix}.$$

Suppose that six UAVs maintain a time-varying hexagon formation from the X-Y plane and retain the rotation around the leader UAV (its dynamic is $[-6\cos(0.025t), 0, t]^T$). Then, $x_i(t)$ and $u_i(t)$ can be rewritten as $x_i(t) = [x_{i\vartheta X}(t), x_{i\vartheta Y}(t), x_{i\vartheta Z}(t), x_{ivX}(t), x_{ivY}(t), x_{ivZ}(t)]^T$, $u_i(t) = [u_{iX}(t), u_{iY}(t), u_{iZ}(t)]^T$, $f_i(t) = [f_{i\vartheta}(t), f_{iv}(t)]^T$, $f_{i\vartheta}(t) = [f_{i\vartheta X}(t), f_{i\vartheta Y}(t), f_{i\vartheta Z}(t)]^T$, $f_{iv}(t) = \dot{f}_{i\vartheta}(t)$. The formation vector $f_{i\vartheta}(t)$ for the ith follower UAV ($i \in \{1,2,3,4,5,6\} \triangleq \mathrm{G}_6$) is given as follows:

$$f_{i\vartheta}(t) = \begin{bmatrix} 4\cos(0.5t + \frac{(i-1)}{3}\pi) \\ 4\sin(0.5t + \frac{(i-1)}{3}\pi) \\ 0 \end{bmatrix}.$$

Then, Fig. 4 will be presented with the position snapshots of the leader and six UAVs.

Set $\phi_1 = 0.02$, $\phi_2 = 0.025$, $\phi_3 = 0.05$, $\phi_4 = 0.045$, $\phi_5 = 0.03$, $\phi_6 = 0.035$. The initial positions of six UAVs are given as $x_{1\vartheta} = [2.5, 1, 2]^T$, $x_{2\vartheta} = [2, 6.4, 4]^T$, $x_{3\vartheta} = [-3, 4.9, 2.4]^T$, $x_{4\vartheta} = [-6.5, 1.5, 4.5]^T$, $x_{5\vartheta} = [-4.8, -2.2, 4.1]^T$, $x_{6\vartheta} = [-1.6, -2.1, 3.3]^T$.

Let $\bar{\delta}_1 = 0.15$, $\bar{\delta}_2 = 0.08$, $\bar{\delta}_3 = 0.1$, $\bar{\delta}_4 = 0.14$, $\bar{\delta}_5 = 0.2$, and $\bar{\delta}_6 = 0.23$, which means that cyber-attacks happen. Choose $M_1 = \mathrm{diag}\{0.15, 0.15, 0.15\}$, $M_2 = \mathrm{diag}\{0.2, 0.2, 0.2\}$, $M_3 = \mathrm{diag}\{0.18, 0.18, 0.18\}$, $M_4 = M_6 = \mathrm{diag}\{0.16, 0.16, 0.16\}$, and $M_5 = \mathrm{diag}\{0.12, 0.12, 0.12\}$ for the attacks such that inequality (8) holds for $\theta = 0$. Then, solving Theorem 2 by MATLAB toolbox follows that

$$\begin{aligned} K_1 =& K_{10} \otimes I_3, K_2 = K_{20} \otimes I_3, \\ K_{10} =& \begin{bmatrix} 0.2213 & 1.0337 \end{bmatrix}, K_{20} = \begin{bmatrix} 0.1045 & 0.4922 \end{bmatrix}, \\ \Omega_\iota =& \Omega_{\iota 0} \otimes I_3, \iota \in \mathrm{G}_6, \\ \Omega_{10} =& \begin{bmatrix} 5.0946 & 0.9697 \\ 0.9697 & 7.6996 \end{bmatrix}, \Omega_{20} = \begin{bmatrix} 4.8600 & 0.2943 \\ 0.2943 & 5.8575 \end{bmatrix}, \end{aligned}$$

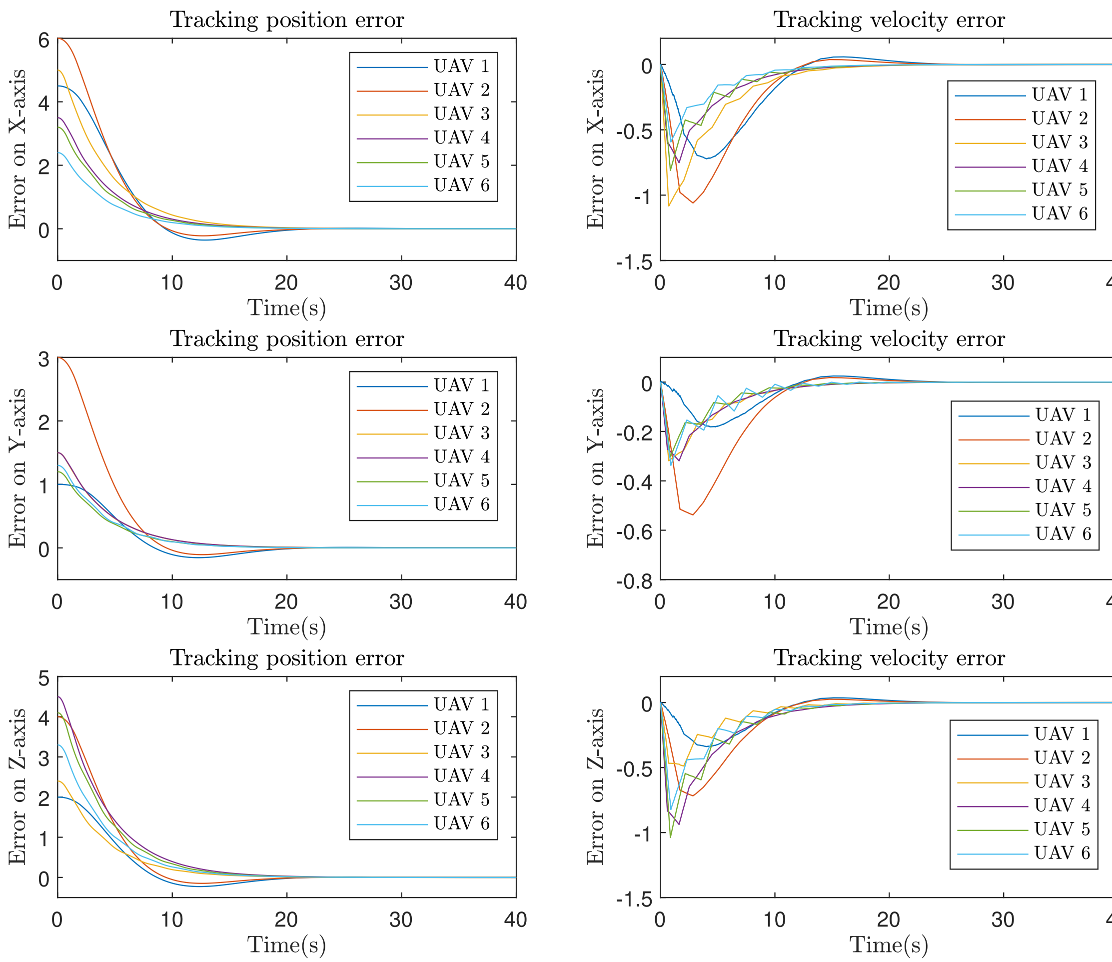

Fig. 3. Tracking errors $\bar{x}(t)$ (including tracking position errors and tracking velocity errors) for six UAVs.

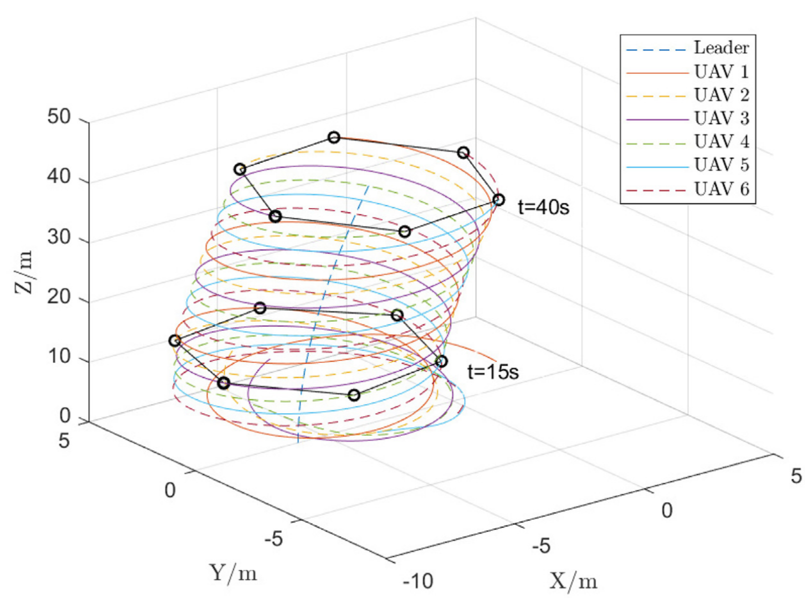

Fig. 4. Position trajectories of the leader and six UAVs, and position snapshots at $t = 15$, 40 s.

$$\Omega_{30} = \begin{bmatrix} 5.2583 & 1.4357 \\ 1.4357 & 9.2583 \end{bmatrix}, \Omega_{40} = \begin{bmatrix} 5.1865 & 1.2510 \\ 1.2510 & 8.6441 \end{bmatrix},$$

$$\Omega_{50} = \begin{bmatrix} 5.0583 & 0.8103 \\ 0.8103 & 7.4407 \end{bmatrix}, \Omega_{60} = \begin{bmatrix} 5.2005 & 1.1971 \\ 1.1971 & 8.5267 \end{bmatrix}.$$

The simulation results for the multi-UAV system are given in Figs. 3–8. The tracking errors $\bar{x}_i(t)$ (including tracking position errors and tracking velocity errors) for six UAVs are exhibited in Fig. 3, from which one can clearly observe that the tracking error

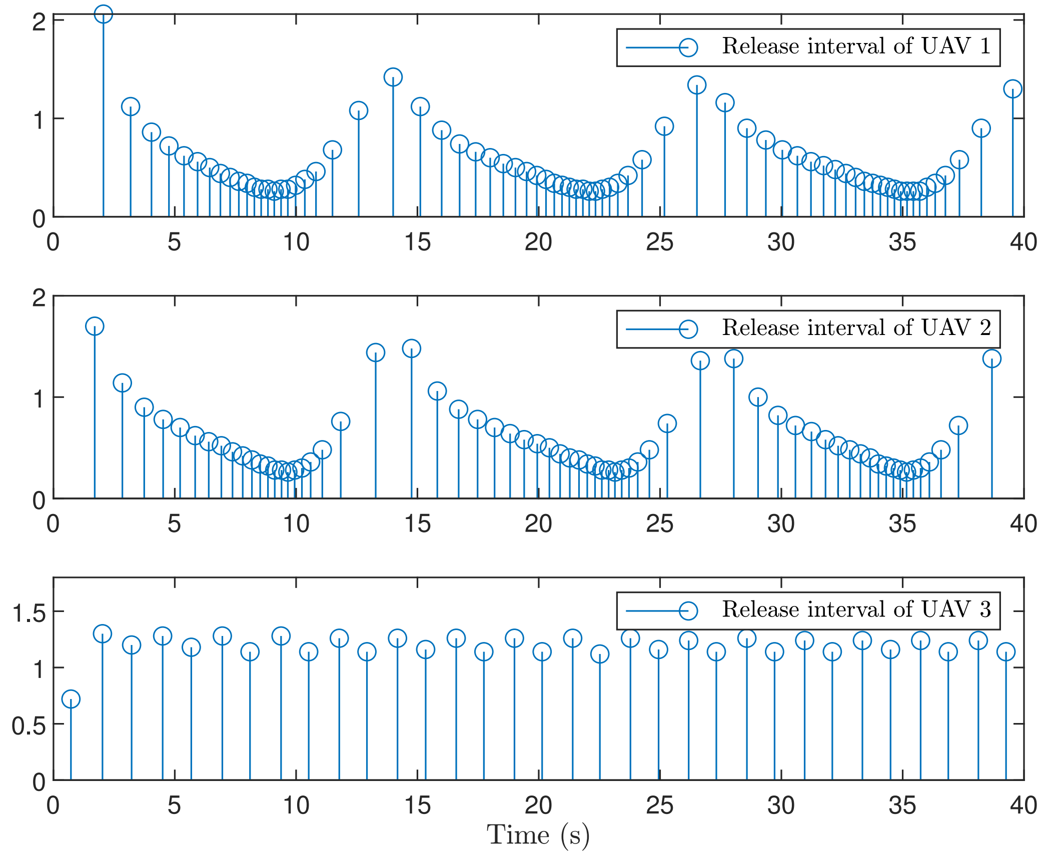

Fig. 5. The TIRIs of UAVs 1–3.

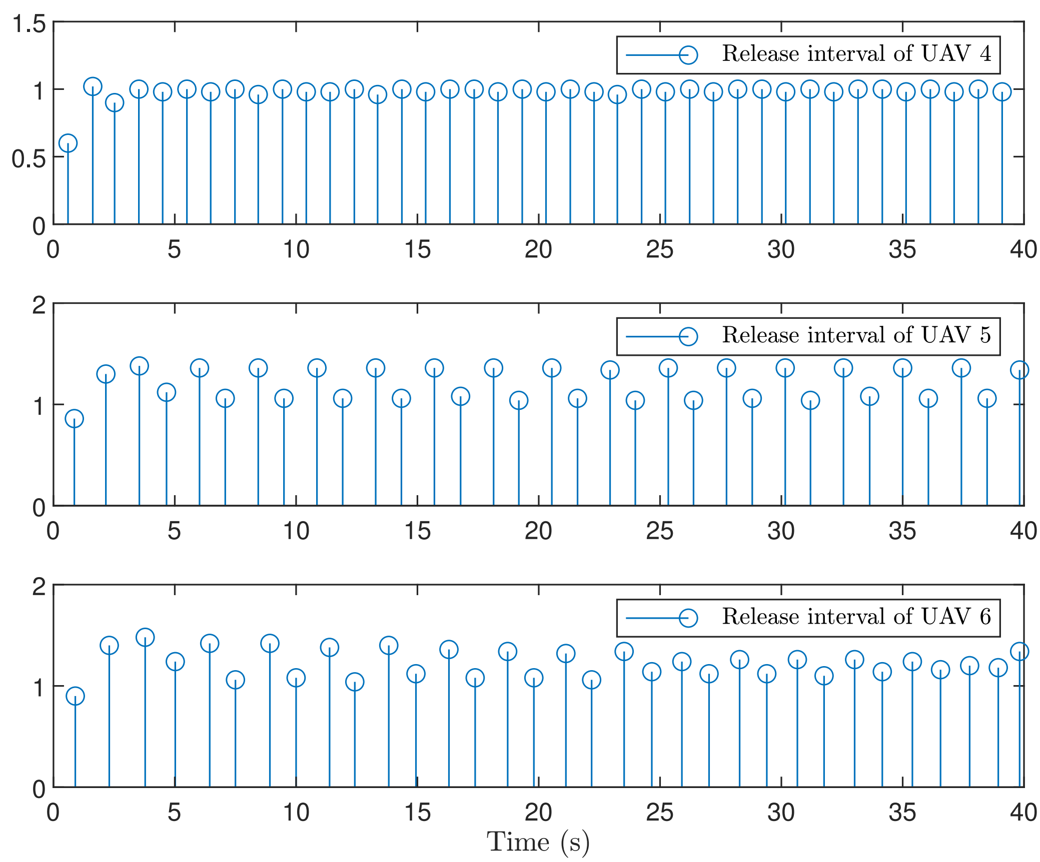

Fig. 6. The TIRIs of UAVs 4–6.

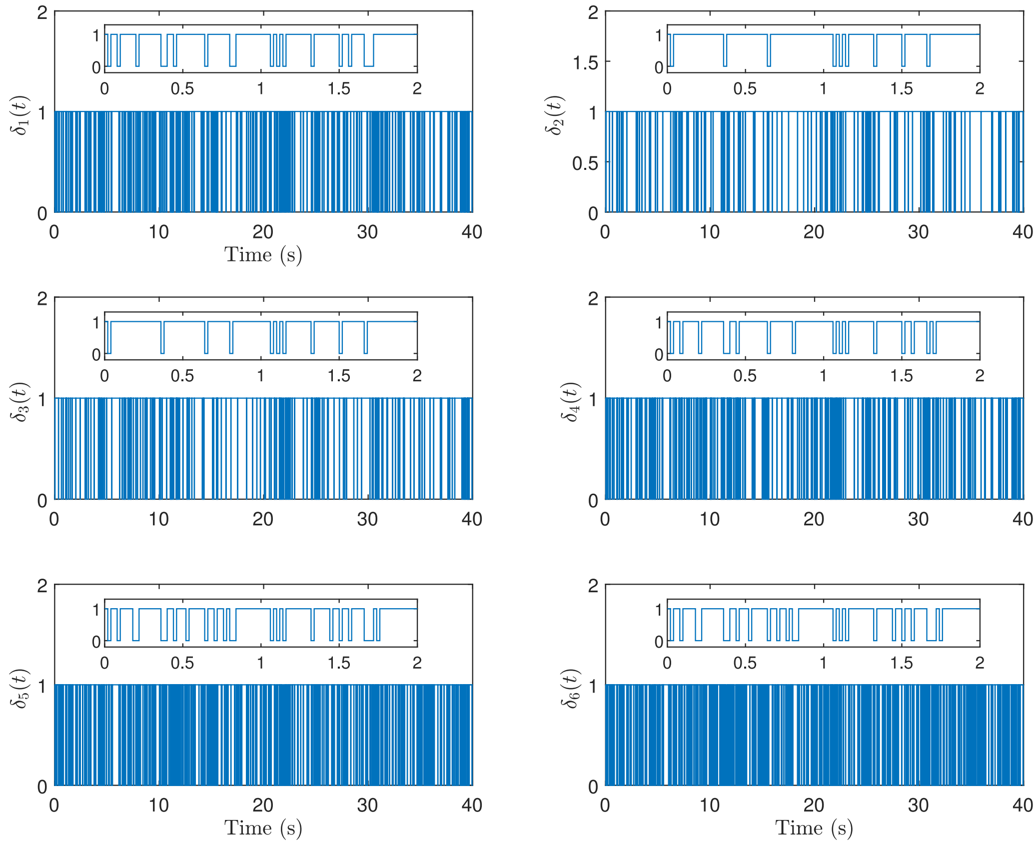

Fig. 7. The distribution of cyber attacks.

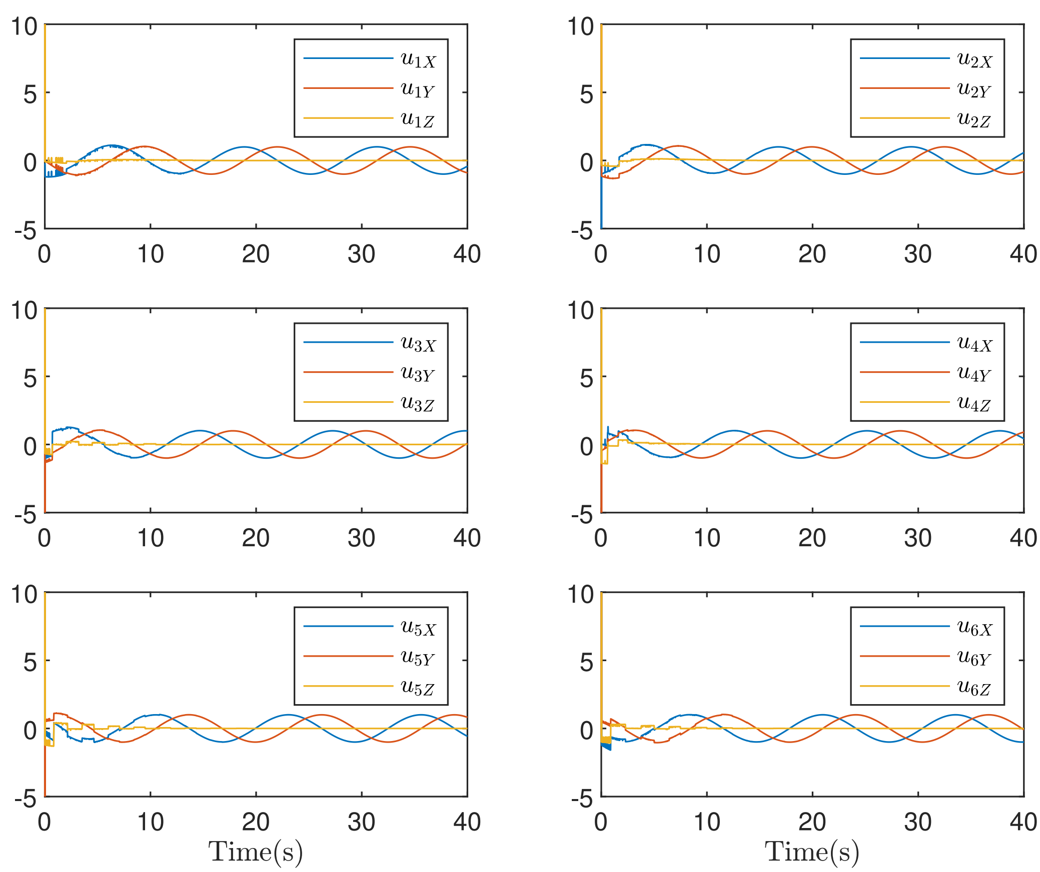

Fig. 8. Real control inputs for six UAVs.

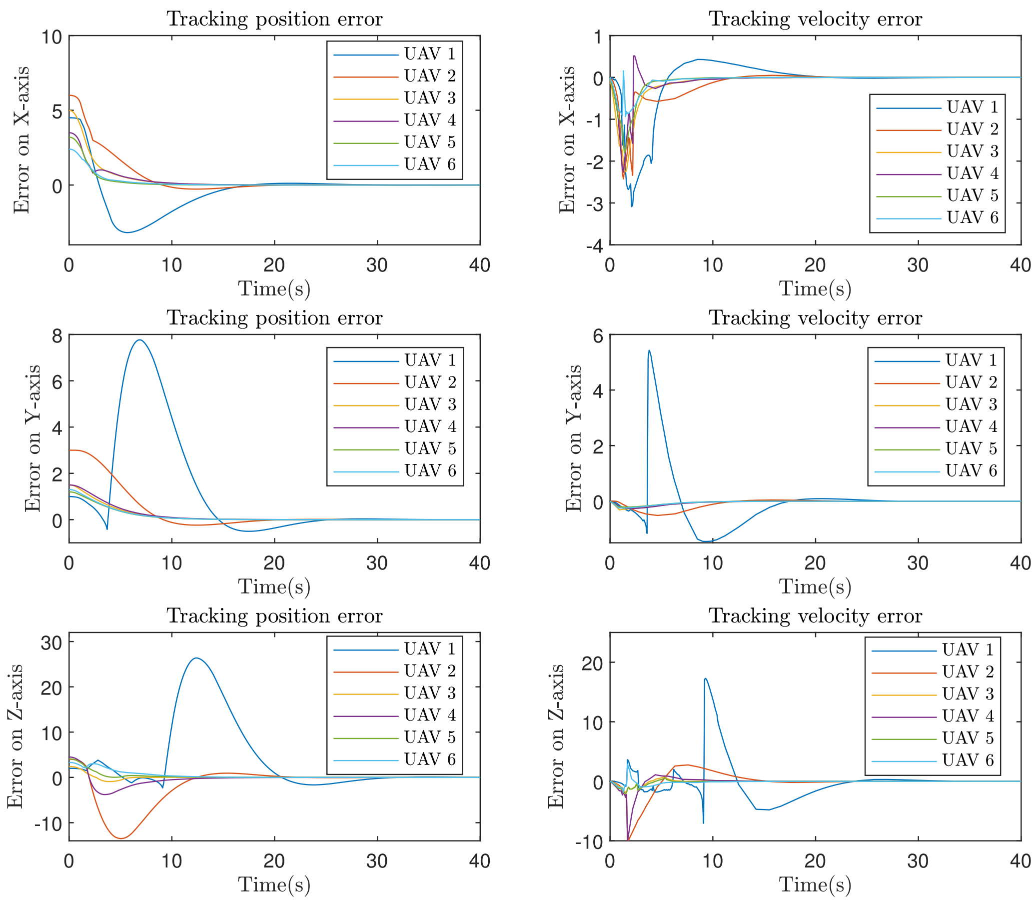

Fig. 9. Tracking errors $\bar{x}(t)$ (including tracking position errors and tracking velocity errors) for six UAVs with the control method in [35].

system of UAVs under cyber-attacks is asymptotically stable. This indicates that each UAV can reach its desired position and complete the formation task. To exhibit the formation transformation more intuitively, the position trajectories of all UAVs are presented in Fig. 4, which also shows the position snapshots at $t = 15, 40$ s.

The triggering instants and releasing intervals (TIRIs) of ETS (4) for six UAVs are shown in Figs. 5–6, from which we notice that the ETS developed in this research can lessen the number of packets releasing by abandoning some redundant data, thus easing the bandwidth load of the communication network among UAVs. Fig. 7 gives the distribution of cyber attacks with $\bar{\delta}_1 = 0.15$, $\bar{\delta}_2 = 0.08$, $\bar{\delta}_3 = 0.1$, $\bar{\delta}_4 = 0.14$, $\bar{\delta}_5 = 0.2$, and $\bar{\delta}_6 = 0.23$. Fig. 8 plots the responses of real control inputs for six UAVs.

To demonstrate the superiority of the proposed formation control method, some comparisons between our developed formation control method and the control methods in [9,35] are given in the following.

Fig. 9 presents tracking errors $\bar{x}(t)$ (including tracking position errors and tracking velocity errors) for six UAVs with the control method in [35] without using a compensation term. By comparing Figs. 3 and 9, one can get that tracking errors in Fig. 3 achieve asymptotically stable in shorter time. This indicates that our proposed control method contributes to shorter time of the multi-UAV system realizing the formation than the control approach in [35] without the compensation term.

Fig. 10 shows the tracking errors $\bar{x}(t)$ (including tracking position errors and tracking velocity errors) for six UAVs with the control method in [9] without cyber-attacks. From Figs. 3 and 10, one can observe that our formation control method brings better control performance of the multi-UAV system under cyber attacks than the control method in [9] without cyber attacks.

Table 1
The NPR of the ith UAV ($i \in \mathcal{G}_6$) within 40 s.

	This study	ETS in [19]	TTCS
NPR of UAV 1	97	465	2000
NPR of UAV 2	82	452	2000
NPR of UAV 3	70	438	2000
NPR of UAV 4	76	446	2000
NPR of UAV 5	71	442	2000
NPR of UAV 6	69	432	2000

In addition, we present a comparison among three communication schemes to further confirm the superiority of our proposed ETS (4), including the ETS in this study, time-triggered communication scheme (TTCS), and the ETS without using the average method in [19]. Under these mechanisms with the same parameter values as above, the number of packets releasing (NPR) of each UAV in the multi-UAV system are recorded within 40 s in Table 1.

In [19] and TTCS, the sampling period is 0.02 s. By comparing the NPR of the ith UAV ($i \in \mathcal{G}_6$) within 40 s in Table 1, one can know that the NPR under our proposed ETS are obviously less than the one under other communication schemes, including the ETS in [19] and the TTCS. This shows that the proposed ETS in this research could improve the energy efficiency and greatly decrease the bandwidth burden of the communication network.

5. Conclusions

This paper has investigated the problem of formation control for multi-UAV systems with cyber attacks using a new ETS with an average method. Under such an ETS, the average of the current

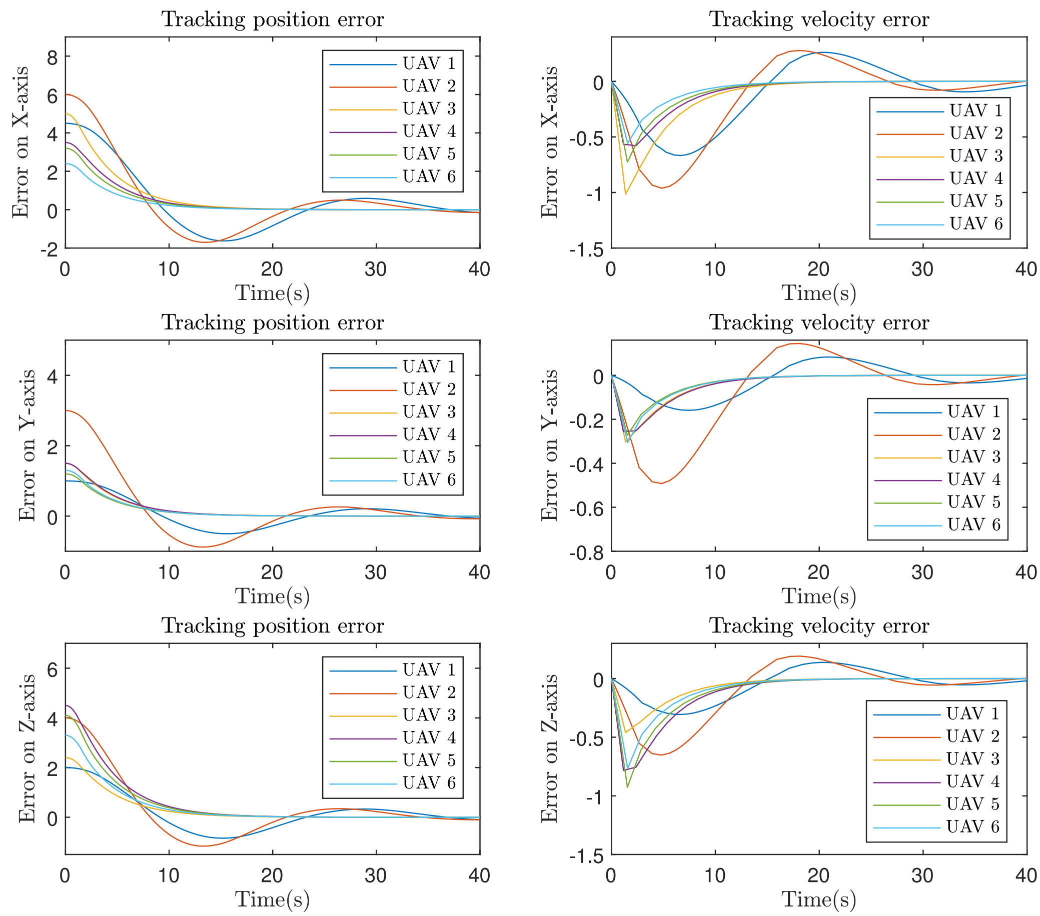

Fig. 10. Tracking errors $\bar{x}(t)$ (including tracking position errors and tracking velocity errors) for six UAVs with the control method in [9].

input signal and the latest triggering signal is applied to design the triggering condition, thus greatly lessening the amount of wrong triggering events caused by the sudden change of system state and saving lots of bandwidth resources. In the presence of cyber attacks, a novel event-based formation control strategy is proposed for multi-UAV systems. Sufficient conditions for the multi-UAV system to realize the desired formation are obtained. Finally, the simulation results affirm the effectiveness of our proposed theoretical method. In the future, we will concern with the research on the attack detection and defense for multi-UAV systems against cyber-attacks, along with some meaningful issues such as obstacle avoidance, nonlinearities and uncertainties, and improved ETSs.

Declaration of competing interest

The authors declare that they have no known competing financial interests or personal relationships that could have appeared to influence the work reported in this paper.

References

[1] Shen Q, Jiang B, Cocquempot V. Fuzzy logic system-based adaptive fault-tolerant control for near-space vehicle attitude dynamics with actuator faults. IEEE Trans Fuzzy Syst 2013;21(2):289–300.
[2] Liu G, Li B, Ji Y. A modified HP-adaptive pseudospectral method for multi-UAV formation reconfiguration. ISA Trans 2022;129:217–29.
[3] Gu Z, Yin T, Ding Z. Path tracking control of autonomous vehicles subject to deception attacks via a learning-based event-triggered mechanism. IEEE Trans Neural Netw Learn Syst 2021;32(12):5644–53.
[4] Wu Y, Low KH. Discrete space-based route planning for rotary-wing UAV formation in urban environments. ISA Trans 2022;129:243–59.
[5] Tian B, Liu L, Lu H, Zuo Z, Zong Q, Zhang Y. Multivariable finite time attitude control for quadrotor UAV: Theory and experimentation. IEEE Trans Ind Electron 2018;65(3):2567–77.
[6] Yin T, Gu Z, Park JH. Event-based intermittent formation control of multi-UAV systems under deception attacks. IEEE Trans Neural Netw Learn Syst Early Access 2022. http://dx.doi.org/10.1109/TNNLS.2022.3227101.
[7] Chen YY, Zhang Y, Liu CL, Wang Q. Formation circumnavigation for unmanned aerial vehicles using relative measurements with an uncertain dynamic target. Nonlinear Dynam 2019;97(4):2305–21.
[8] Guo K, Li X, Xie L. Ultra-wideband and odometry-based cooperative relative localization with application to multi-UAV formation control. IEEE Trans Cybern 2020;50(6):2590–603.
[9] Wei L, Chen M, Li T. Dynamic event-triggered cooperative formation control for UAVs subject to time-varying disturbances. IET Control Theory Appl 2020;14(7):2514–25.
[10] Dong X, Zhou Y, Ren Z, Zhong Y. Time-varying formation tracking for second-order multi-agent systems subjected to switching topologies with application to quadrotor formation flying. IEEE Trans Ind Electron 2017;64(6):5014–24.
[11] Wang J, Han L, Dong X, Li Q, Ren Z. Distributed sliding mode control for time-varying formation tracking of multi-UAV system with a dynamic leader. Aerosp Sci Technol 2021;111:106549.
[12] He L, Bai P, Liang X, Zhang J, Wang W. Feedback formation control of UAV swarm with multiple implicit leaders. Aerosp Sci Technol 2018;72:327–34.
[13] Zhang Y, Feng J, Zhao D, Yan XG, Spurgeon SK. Consensus control for a class of linear multiagent systems using a distributed integral sliding mode strategy. J Franklin Inst 2022;359(2):1086–111.
[14] Liu J, Yin T, Cao J, Yue D, Karimi HR. Security control for T–S fuzzy systems with adaptive event-triggered mechanism and multiple cyber-attacks. IEEE Trans Syst Man Cybern Syst 2021;51(10):6544–54.
[15] Gu Z, Ahn CK, Yan S, Xie X, Yue D. Event-triggered filter design based on average measurement output for networked unmanned surface vehicles. IEEE Trans Circuits Syst II Express Briefs 2022;69(9):3804–8.

[16] Xie X, Wan L, Gu Z, Yue D, Sun J. Enhanced resilient fuzzy stabilization of discrete-time Takagi–Sugeno systems based on augmented time-variant matrix approach. IEEE Trans Cybern Early Access 2022. http://dx.doi.org/10.1109/TCYB.2022.3179048.

[17] Hu S, Yue D, Yin X, Xie X, Ma Y. Adaptive event-triggered control for nonlinear discrete-time systems. Internat J Robust Nonlinear Control 2016;26(18):4104–25.

[18] Yan S, Gu Z, Park JH, Xie X. Synchronization of delayed fuzzy neural networks with probabilistic communication delay and its application to image encryption. IEEE Trans Fuzzy Syst Early Access 2022. http://dx.doi.org/10.1109/TFUZZ.2022.3193757.

[19] Yan S, Shen M, Nguang SK, Zhang G. Event-triggered H_∞ control of networked control systems with distributed transmission delay. IEEE Trans Automat Control 2020;65(10):4295–301.

[20] Zheng S, Shi P, Agarwal RK, Lim CP. Periodic event-triggered output regulation for linear multi-agent systems. Automatica 2020;122:109223.

[21] Chen M, Yan H, Zhang H, Chi M, Li Z. Dynamic event-triggered asynchronous control for nonlinear multi-agent systems based on T–S fuzzy models. IEEE Trans Fuzzy Syst 2021;29(9):2580–92.

[22] Zhao Y, Xian C, Wen G, Huang P, Ren W. Design of distributed event-triggered average tracking algorithms for homogeneous and heterogeneous multi-agent systems. IEEE Trans Automat Control 2022;67(3):1269–84.

[23] Wang A, Mu B, Shi Y. Consensus control for a multi-agent system with integral-type event-triggering condition and asynchronous periodic detection. IEEE Trans Ind Electron 2017;64(7):5629–39.

[24] Zhao G, Hua CC. A hybrid dynamic event-triggered approach to consensus of multi-agent systems with external disturbances. IEEE Trans Automat Control 2021;66(7):3213–20.

[25] Yue D, Tian E, Han Q. A delay system method for designing event-triggered controllers of networked control systems. IEEE Trans Automat Control 2013;58(2):475–81.

[26] Tian E, Peng C. Memory-based event-triggering H_∞ load frequency control for power systems under deception attacks. IEEE Trans Cybern 2020;50(11):4610–8.

[27] Gu Z, Shi P, Yue D, Yan S, Xie X. Memory-based continuous event-triggered control for networked T–S fuzzy systems against cyber-attacks. IEEE Trans Fuzzy Syst 2021;29(10):1570–9.

[28] Zou L, Wang Z, Zhou D. Moving horizon estimation with non-uniform sampling under component-based dynamic event-triggered transmission. Automatica 2020;120:109154.

[29] Gu Z, Ahn CK, Yue D, Xie X. Event-triggered H_∞ filtering for T–S fuzzy-model-based nonlinear networked systems with multisensors against DoS attacks. IEEE Trans Cybern 2022;52(6):5311–21.

[30] Liu J, Zhang N, Li Y, Xie X. H_∞ filter design for discrete-time networked systems with adaptive event-triggered mechanism and hybrid cyber attacks. J Franklin Inst 2021;358(17):9325–45.

[31] Sun X, Gu Z, Yang F, Yan S. Memory-event-trigger-based secure control of cloud-aided active suspension systems against deception attacks. Inform Sci 2021;543:1–17.

[32] Zhu JW, Yang YP, Zhang WA, Yu L, Wang X. Cooperative attack tolerant tracking control for multi-agent system with a resilient switching scheme. Neurocomputing 2020;409:372–80.

[33] Xie X, Yue D, Zhang H, Xue Y. Fault estimation observer design for discrete-time Takagi–Sugeno fuzzy systems based on homogenous polynomially parameter-dependent Lyapunov functions. IEEE Trans Cybern 2017;47(9):2504–13.

[34] Yin T, Gu Z, Xie X. Observer-based event-triggered sliding mode control for secure formation tracking of multi-UAV systems. IEEE Trans Netw Sci Eng Early Access 2022. http://dx.doi.org/10.1109/TNSE.2022.3223978.

[35] Wu Z, Cao J, Wang Y, Wang Y, Zhang L, Wu* J. hPSD: A hybrid PU-learning-based spammer detection model for product reviews. IEEE Trans Cybern 2020;50(4):1595–606.

[36] Ye D, Zhang TY, Guo G. Stochastic coding detection scheme in cyber–physical systems against replay attack. Inform Sci 2019;481:432–44.

[37] Fang C, Qi Y, Cheng P, Zheng WX. Optimal periodic watermarking schedule for replay attack detection in cyber–physical systems. Automatica 2020;112:108698.

[38] Chen B, Ho DW, Hu G, Yu L. Secure fusion estimation for bandwidth constrained cyber–physical systems under replay attacks. IEEE Trans Cybern 2017;48(6):1862–76.

[39] Zhu M, Martínez S. On the performance analysis of resilient networked control systems under replay attacks. IEEE Trans Automat Control 2014;59(3):804–8.

[40] Yuan H, Xia Y, Yang H, Yuan Y. Resilient control for wireless networked control systems under DoS attack via a hierarchical game. Internat J Robust Nonlinear Control 2018;28(15):4604–23.

[41] Xu Y, Fang M, Wu ZG, Pan YJ, Chadli M, Huang T. Input-based event-triggering consensus of multiagent systems under denial-of-service attacks. IEEE Trans Syst Man Cybern Syst 2018;50(4):1455–64.

[42] Zhang TY, Ye D. Distributed event-triggered control for multi-agent systems under intermittently random denial-of-service attacks. Inform Sci 2021;542:380–90.

[43] Shao X, Ye D. Neural-network-based adaptive secure control for nonstrict-feedback nonlinear interconnected systems under DoS attacks. Neurocomputing 2021;448:263–75.

[44] Zhang Z, Dong J. Fault-tolerant containment control for IT2 fuzzy networked multiagent systems against denial-of-service attacks and actuator faults. IEEE Trans Syst Man Cybern Syst 2022;52(4):2213–24.

[45] Yang F, Gu Z, Hua L, Yan S. A resource-aware control approach to vehicle platoons under false data injection attacks. ISA Trans 2022;131:367–76.

[46] Liu L, Sun H, Ma L, Zhang J, Bo Y. Quasi-consensus control for a class of time-varying stochastic nonlinear time-delay multiagent systems subject to deception attacks. IEEE Trans Syst Man Cybern Syst 2021;51(11):6863–73.

[47] Wen G, Zhai X, Peng Z, Rahmani A. Fault-tolerant secure consensus tracking of delayed nonlinear multi-agent systems with deception attacks and uncertain parameters via impulsive control. Commun Nonlinear Sci Numer Simul 2020;82:105043.

[48] He W, Gao X, Zhong W, Qian F. Secure impulsive synchronization control of multi-agent systems under deception attacks. Inform Sci 2018;459:354–68.

[49] He W, Mo Z. Secure event-triggered consensus control of linear multi-agent systems subject to sequential scaling attacks. IEEE Trans Cybern 2022;52(10):10314–27.